Journal of Magnetic Resonance 204 (2010) 155–159

Contents lists available at ScienceDirect

Journal of Magnetic Resonance

journal homepage: www.elsevier.com/locate/jmr

Communication

Structural study of the membrane protein MscL using cell-free expression and solid-state NMR

Alaa Abdine [a], Michiel A. Verhoeven [a,b], Kyu-Ho Park [c,1], Alexandre Ghazi [c], Eric Guittet [b], Catherine Berrier [c], Carine Van Heijenoort [b], Dror E. Warschawski [a,*]

[a] UMR 7099, CNRS and Université Paris Diderot, IBPC, 13 rue Pierre et Marie Curie, F-75005 Paris, France
[b] UPR 2301, CNRS, ICSN, F-91190 Gif-sur-Yvette, France
[c] UMR 8619, CNRS and Université Paris-Sud 11, IBBMC, F-91405 Orsay, France

ARTICLE INFO

Article history:
Received 25 December 2009
Revised 1 February 2010
Available online 11 February 2010

Keywords:
Solid-state NMR spectroscopy
Magic-angle spinning
Membrane proteins
Isotope labeling
Structural biology

ABSTRACT

High-resolution structures of membrane proteins have so far been obtained mostly by X-ray crystallography, on samples where the protein is surrounded by detergent. Recent developments of solid-state NMR have opened the way to a new approach for the study of integral membrane proteins *inside* a membrane. At the same time, the extension of cell-free expression to the production of membrane proteins allows for the production of proteins tailor made for NMR. We present here an *in situ* solid-state NMR study of a membrane protein selectively labeled through the use of cell-free expression. The sample consists of MscL (mechano-sensitive channel of large conductance), a 75 kDa pentameric α-helical ion channel from *Escherichia coli*, reconstituted in a hydrated lipid bilayer. Compared to a uniformly labeled protein sample, the spectral crowding is greatly reduced in the cell-free expressed protein sample. This approach may be a decisive step required for spectral assignment and structure determination of membrane proteins by solid-state NMR.

1. Introduction

In recent years, solid-state NMR has shown its efficiency on studying microcrystalline soluble proteins in the solid-state [1–3], and it is now applied to molecules that must be studied by solid-state NMR in their native state, like fibrils [4–6], macromolecular assemblies [7] and membrane proteins in a lipid environment [8–15]. In the latter case, spectral resolution remains a crucial issue, first because the local order of proteins inserted in lipid bilayers is often not as high as that of micro-crystals and second, because membrane proteins are often composed of repetitive hydrophobic amino acids in α-helices. Spectral congestion can be overcome by removing a number of resonances from the NMR spectra, by isotopically labeling only a subset of the protein nuclei, through different biochemical methods [1,4,13,16,17]. Another major challenge is the production of large quantity of functional proteins. The cytotoxicity of overexpression is aggravated, in the case of membrane proteins, by the limited membrane surface available. The recently developed cell-free expression (CFE) approach for protein production is particularly well adapted for selective labeling of amino acids, and it has proven its efficiency in solution-state NMR studies [18–21]. It is applied here to a solid-state NMR study, where it will be even more useful due to crucial spectral crowding issues.

In this communication, we also present the first NMR study of the mechano-sensitive channel of large conductance from *E. coli* (MscL), a 75 kDa homopentameric membrane protein that functions as a pressure valve in the bacterial inner membrane. While the structure of a closed form of the analogous Tb-MscL pentamer from *Mycobacterium tuberculosis* has been determined by X-ray crystallography [22], the opening/closing of the channel can only occur when the protein is embedded in a lipid bilayer [23]. Furthermore, the recent structure determination of a *tetrameric* analog from *Staphylococcus aureus* [24] shows an unexpected structural variety of these ion channels, and has revived the interest for the structure determination of membrane proteins in their native environment.

2. Results

Small scale cell-free expression of functional MscL in the presence of detergents has been optimized before [25]. By scaling up this protocol, we have synthesized several milligrams of MscL ^{13}C, ^{15}N-labeled on the 16 isoleucine and on the 3 threonine residues. The high repetition of isoleucines makes them a good probe

* Corresponding author. Fax: +33 1 58 41 50 24.
E-mail address: Dror.Warschawski@ibpc.fr (D.E. Warschawski).
[1] Present address: URA 3015, CNRS and Institut Pasteur, Département de Virologie, 25 rue du Dr. Roux, F-75015 Paris, France.

1090-7807/$ - see front matter © 2010 Elsevier Inc. All rights reserved.
doi:10.1016/j.jmr.2010.02.003

for resolution, whereas the low amount of threonines is a good test for sensitivity. For comparison, we have also prepared a uniformly ^{13}C, ^{15}N-labeled MscL sample by expression in *E. coli*. After purification, reconstitution of MscL is feasible in a large number of lipid mixtures and we have obtained NMR spectra in DOPC, DOPC/DPPC and soybean asolectin, with several lipid-to-protein ratios. Since the resolution was the same (data not shown), the data presented here corresponds to MscL reconstituted in a DOPC membrane, in which it is as active as in a natural membrane [26].

The state of our proteoliposomes was checked by several approaches: (i) crosslinking experiments with formaldehyde and disuccinyl suberate showed the integrity of the pentamer on SDS–PAGE gel; (ii) sucrose flotation on a discontinuous sucrose gradient of 50/30/20/0% (before and after washing them with urea, to exclude proteins that would merely sit on the membrane surface), resulted in a single band at the interface of 20–30% corroborating protein charged liposomes; (iii) ^{31}P NMR at room temperature resulted in a typical hydrated fluid bilayer spectrum; (iv) electron microscopy resulted in a typical proteoliposome picture with no signs of protein precipitation; (v) the functionality of the proteins was assayed using standard patch–clamp methods [25]; (vi) finally, ^{1}H and ^{13}C NMR spectra were acquired prior to and after each NMR set of experiments and showed no sign of dehydration or lipid degradation.

With a sample typically containing 3 mg of proteins, 12 mg of lipids and 50% (w/w) of water, a 1D ^{13}C solid-state NMR spectrum can be obtained in about an hour (Fig. 1). Spectral crowding in the C′ (160–180 ppm) and Cα (40–60 ppm) regions is important (Fig. 1a). The 1D spectrum of MscL specifically labeled through CFE, recorded and processed with identical parameters is shown in Fig. 1b. The sensitivity of this spectrum is satisfactory since threonine residues are visible in the CαCβ region (55–70 ppm). In addition, crowding reduction clearly improves the spectral reading, as predicted by the simulations (see Fig. S1 in the Supplementary Data, SD).

Protein structural studies by solid-state NMR rely on 2D ^{13}C–^{13}C spectra where the first limiting step consists in assigning resonances coming from each residue. Fig. 2 shows the comparison of 2D ^{13}C–^{13}C solid-state NMR spectra, obtained through the DARR experiment [27], on both samples described previously: MscL either uniformly ^{13}C and ^{15}N labeled produced in *E. coli* (Fig. 2a) or selectively ^{13}C and ^{15}N labeled by CFE on all isoleucine and threonine residues (Fig. 2b), both reconstituted in a hydrated lipid bilayer. The current spectral resolution does not allow the assignment of over 700 different carbons, as seen in Fig. 2a. As expected, since the specifically labeled sample contains only 108 ^{13}C spins, the corresponding spectra appear spectacularly less congested. With the same acquisition parameters, the CαCβ threonine resonances are visible in Fig. 2b, while they are buried in the noise in Fig. 2a (they can be distinguished with longer acquisition times, see Fig. S2 in the SD).

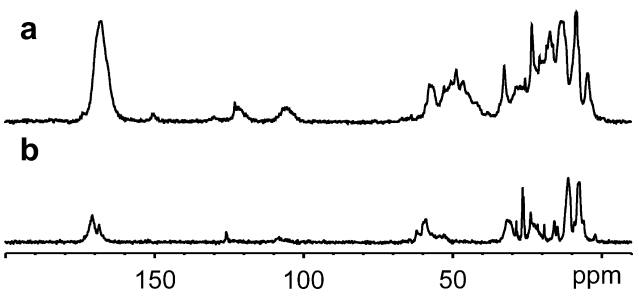

Fig. 1. 176 MHz 1D ^{13}C CP MAS NMR spectra of labeled MscL in unlabeled DOPC liposomes, spinning at 11,000 Hz and 258 K: (a) U-^{13}C, ^{15}N labeled and (b) (Ile, Thr)-^{13}C, ^{15}N labeled.

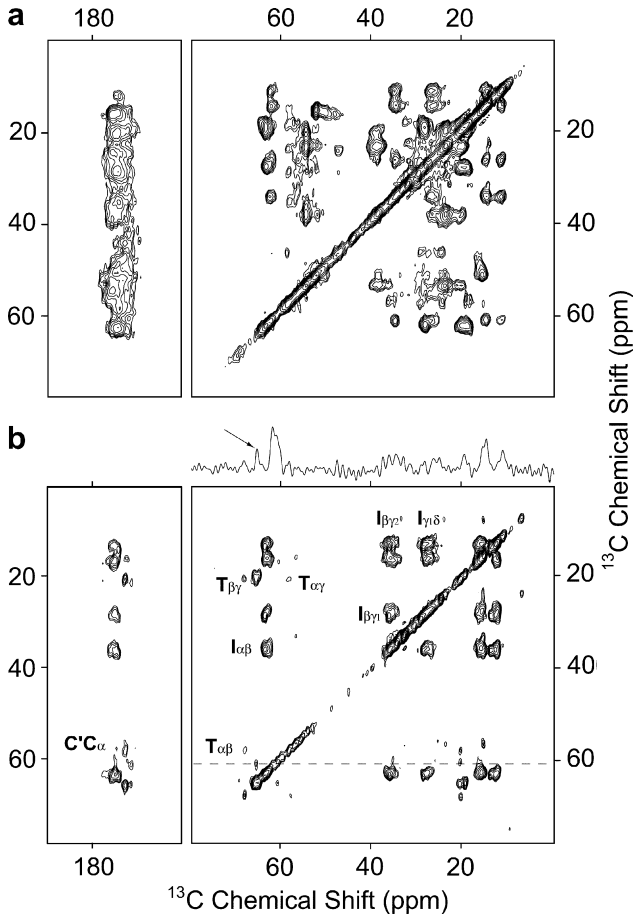

Fig. 2. 2D ^{13}C–^{13}C DARR NMR (50 ms mixing time, 14 h of acquisition) spectra of MscL/DOPC: (a) U-^{13}C, ^{15}N labeled protein and (b) (Ile, Thr)-^{13}C, ^{15}N labeled protein, with a cross section through the threonine αβ region shown on top. The arrow indicates a threonine cross signal which is 140 Hz wide (0.80 ppm). Some unlabeled lipid signals appear on the diagonal, mostly around 30 ppm.

The DARR experiment was performed at several mixing times between 5 and 500 ms to monitor the build-up of each correlation. At 500 ms, long range cross signals between isoleucines and threonines could be observed in the selectively labeled sample (see Fig. 3). Since there is no adjacent isoleucine–threonine pair in MscL, this opens the way for future long distance measurements and structure determination.

3. Discussion

In vitro synthesis offers a good alternative to biosynthesis. With a good yield and a very simple purification step, our membrane protein can be cell-free expressed in 2 days, as opposed to 8 days in *E. coli*. Moreover, for a moderate number of labeled amino acids (up to 5), the cost of a CFE sample is comparable to that of a uniformly labeled sample produced *in vivo*, and much less than that of a specifically labeled *in vivo* sample. Finally, CFE bypasses cytotoxicity and membrane targeting issues, as well as greatly minimizing amino acid scrambling.

In all cases, our proteins are well folded, as shown by various biochemical and biophysical tests described above in the Section 2. Our sample is also homogeneous, as confirmed by the presence of narrow individual resonances (see for example the cross sections at 60.7 ppm on Fig. 2b and Fig. S2 in the SD), comparable to recently published spectra [13]. There are very few such individual resonances because the hydrophobic residues are all in a similar

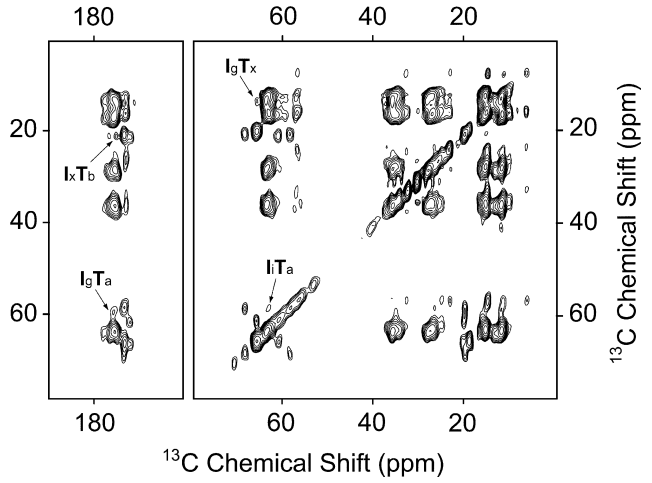

Fig. 3. 2D ^{13}C–^{13}C DARR NMR (500 ms mixing time, total experiment time: 56 h) spectra of (Ile, Thr)-^{13}C, ^{15}N labeled MscL/DOPC. Some long range cross signals are indicated on the spectrum (Ix and Tx indicate that the specific isoleucine or threonine could not be identified).

chemical environment. The resolution is sufficient to fully characterize the 3 threonine sets of spin systems. In the case of the 16 isoleucine residues of MscL, up to 10 different sets of spin systems can be distinguished (see Figs. S3 and S4 and Tables S1 and S2 in the SD).

Crowding reduction by CFE results from the reduced number of spins and spin couplings. For instance, the specifically labeled sample contains less ^{13}C–^{13}C pairs of spins from neighboring residues, which modifies the interactions, spin diffusion and relaxation experienced by the remaining spins. Long-range contacts in the specifically labeled sample will thereby suffer less from relayed polarization transfers in correlation experiments, hence resulting in potentially more accurate deduced distances.

MscL is a good candidate for testing various assignment strategies in solid-state NMR because it contains a high percentage (40%) of hydrophobic residues. Clearly, sequential information is required to assign the resonances. While isotopic labeling of a small number of amino acids reduces the probability of adjacent amino acid pairs that are required for sequential assignment, larger well-chosen sets of labeled amino acids will allow access to complete assignment, using ^{13}C and ^{15}N NMR. Several ways can be followed, inspired from solution-state NMR studies: the combinatorial approach suggested by the Otting group [18] or the "dual combinatorial" approach of the Dotsch group [20]. Both approaches will have to be adapted to the particular case of solid-state NMR where carbons and nitrogens are observed, rather than protons, and where the dipolar interaction dominates the scalar one. Another labeling strategy could focus solely on amino acids that are important for the channel function [19,28], and CFE will become a necessity for the study of potential open mutants that would be lethal for bacterial growth. Finally, knowing the structure of a model [29] or an analog of our protein, an approximate NMR spectrum can be simulated, using for example the SPARTA package [30]. This simulated spectrum can, in turn, help us choose an efficient labeling strategy that would minimize the spectral overlap [31]. Regardless, the required specific labeling is most efficiently achieved by CFE and we demonstrate the feasibility of this strategy in combination with solid-state NMR.

4. Conclusions

Combined with new technological developments, such as Dynamic Nuclear Polarization, cryo-NMR or very high fields, solid-state NMR is currently adapting to the study of larger molecules, where both high-resolution and high sensitivity are still challenges to attain. We have shown here that our CFE approach is efficient to simplify an overcrowded NMR spectrum and that it provides a useful approach for the first steps of assigning membrane proteins by solid-state NMR. It is competitive and complementary to other labeling schemes that have been suggested to alleviate assignment obstacles. We also expect our strategy to be very helpful to extract secondary structure and dynamics information, as well as distance constraints and thus for structure determination by solid-state NMR. Solid-state NMR, together with novel biochemistry techniques for protein isotopic labeling, is an efficient technique for studying the ion channel MscL inside a hydrated lipid bilayer. Such an approach is very general and should therefore be applicable to other channels or membrane protein structural studies.

5. Experimental

5.1. Membrane protein expression

The *mscL* gene with a C-terminal His_6-Tag, cloned under the T7 promoter into pIVEX2.3 plasmid was used [25]. The recombinant plasmid was introduced in the *E. coli* BL21(λDE3) strain (Stratagene) by electroporation. Precultures were grown overnight in LB medium, which was removed by centrifugation (5000*g*, 4 °C, 20 min) before inoculation of selective M9 medium (3 L with 100 μg/mL ampicillin) containing $^{13}C_6$-glucose (3 g/L) and ^{15}N-ammonium chloride (1 g/L, Spectra Stable Isotopes). Cultures were grown in shaking bottles at 37 °C. When the optical density at 600 nm reached 0.6–0.8, protein expression was induced for 3 h by 1 mM IPTG (Sigma–Aldrich). Cells were harvested by centrifugation and stored overnight at −20 °C. The bacterial pellet was resuspended in buffer (50 mM NaH_2PO_4, 10 mM NaCl, 2 mM $MgSO_4$, 5% sucrose, 1 mM phenylmethylsulphonyl fluoride, 10 μg/mL DNase, 2 mM mercapto ethanol, 1 mM dithiothreitol), cells were broken using a French press at 10^4 psi (twice). Cell debris were removed by centrifugation (5000*g*, 4 °C, 20 min) and membranes were isolated by ultra-centrifugation (300,000*g*, 4 °C, 30 min). The membrane pellet was resuspended for 30 min at room temperature in buffer A (50 mM Na_2HPO_4, pH 7, 200 mM NaCl) containing 2% Triton X-100 and 10 mM imidazole. Unsolubilized material was discarded by a second ultra-centrifugation (300,000*g*, 4 °C, 30 min) and the supernatant was immediately purified on an affinity column.

In vitro expression of MscL was performed with the RTS9000 kit (Roche) in combination with the Amino Acid Sampler (Roche) as follows: 150 μg of plasmid were incubated for 23 h at 30 °C in the presence of the lysate containing 31 and 35 mg of uniformly ^{13}C, ^{15}N-labeled Thr and Ile respectively (Spectra Stable Isotopes), while the remaining 18 unlabeled amino acids were added from the Amino Acid Sampler. Although a large variety of non ionic detergents could be used [29], Triton X-100 was added in a final concentration of 0.2% in a final reaction volume of 10 mL. At the end of the run, the reaction mixture was diluted 5 times in buffer A containing 1% Triton and centrifuged (5000*g*, 4 °C, 15 min) to remove precipitates before FPLC purification. Recent progress in CFE efficiency suggests that the amount of amino acids added could be cut by a factor of 6 (A. Pedersen, private communication), and the lysate could be home made, reducing the cost by an additional significant factor.

5.2. Protein purification and membrane reconstitution

FPLC chromatography of the His_6-tagged MscL was performed using a 1 mL Ni^{2+} charged HiTrap chelating HP column (GE). After removal of unbound material, Triton X-100 concentration was adjusted to 0.2% if necessary. Unspecifically bound material was

washed out using buffer A supplemented with 100 mM imidazole, and MscL was eluted at a concentration of 500 mM imidazole. In order to reduce the imidazole concentration, the fractions containing the protein were pooled and dialysed twice against 1 L of buffer B (10 mM HEPES KOH, pH 7.4, 100 mM KCl, 0.2% Triton X-100), using a dialysis cassette (Pierce) with a cut-off value of 10 kD. The amount of produced proteins was quantified with the Micro-BCA kit (Pierce) and indicated a yield of ~1 mg/L for the sample produced *in vivo* and 800 μg/mL for the sample produced *in vitro*.

The buffer containing purified MscL was combined with buffer B containing DOPC/Triton mixed micelles to achieve a final lipid/detergent ratio of 1/3 and a lipid/protein ratio of 4/1 (w/w). The detergent (~12 mg) was then removed by addition of twice 120 mg of SM2-BioBeads as described before [32]. The proteoliposomes were pelleted (300,000 g, 4 °C, 30 min) and transferred into 50 μL 4 mm NMR rotors (Bruker) and stored at −20 °C until used for data acquisition. Several other sample conditions were tested, using DOPC/DPPC:1/1 (Avanti) or soybean asolectin (Fluka), and lipid/protein ratios from 4/1 to 1/1 (w/w). The phospholipid content of the sample was checked by the method of Rouser [33]. Water content was estimated by weighing samples produced in parallel prior to and after 16 h in vacuum.

5.3. NMR

Solid-state NMR experiments were run on a Bruker 700 MHz spectrometer using a triple resonance 4 mm MAS probe. ^{13}C chemical shifts were referenced relative to adamantane as a secondary reference [34]. Reducing the temperature may improve spectral resolution and sensitivity by increasing Boltzmann polarization, freezing molecular motion and improving the efficiency of sample-spinning, proton decoupling and cross polarization. On the other hand, dipolar couplings and T_1 relaxation times are increased, and multiple conformations are frozen out, resulting in potentially broader lines [8,10,14]. Samples were maintained at 258 K for the duration of the measurements at a sample-spinning rate of 11,000 Hz (±3 Hz). The temperature inside the spinning rotor was checked by measuring the transition temperature of DOPC in the same conditions. Several experiments were performed at higher temperatures (288 K), and did not give a better spectral resolution (data not shown). At comparable resolution, experiments were therefore performed at a lower temperature to extend the lifetime of the protein.

1D ^{13}C MAS NMR experiments were performed with ramped CP (1.5 ms contact time and rf power of 50 kHz), TPPM ^{1}H decoupling (rf power of 100 kHz), 1024 scans and 4 s repetition time. 2D ^{13}C–^{13}C correlation experiments were performed using the analogous DARR or PDSD experiments [27,35,36] with similar ramped CP and TPPM ^{1}H decoupling during indirect evolution and acquisition periods. ^{1}H and ^{13}C rf powers were 100 and 50 kHz respectively, except for the ^{1}H DARR mixing pulse set at 11 kHz (equal to the spinning rate), and varied between 5 and 500 ms. Sampling parameters were 10 μs for 2048 points (direct dimension) by 10 μs for 256 rows (indirect dimension), with 64 scans per row and 3 s repetition time. Total time was approximately 14 h. A few experiments were conducted with 256 scans per row, amounting to 56 h acquisition time. Data were processed with nmrPipe [37], employing zero filling and 90° shifted sine bell apodization in the indirect dimension, 10 Hz exponential line broadening in the direct dimension and automatic baseline correction in both dimensions. Only the positive contours are displayed.

Acknowledgments

This work was supported by a fellowship from the Ministère de l'Enseignement Supérieur et de la Recherche (to A.A.), grants and post-doctoral fellowships (to M.V. and K.-H.P.) by the CNRS (UMR 7099, UPR 2301, UMR 8619), the ANR (ANR-06-JCJC0014), the Université Paris Diderot and the Université Paris-Sud. We thank Daniel Lévy for the electron microscopy, Cathy Etchebest for the molecular dynamics simulations, Philippe Devaux and Francesca Zito for stimulating scientific discussions.

Appendix A. Supplementary data

1D ^{13}C NMR simulations of MscL (Fig. S1), long 2D ^{13}C–^{13}C PDSD NMR spectrum of U-^{13}C labeled MscL (Fig. S2), zooms in the 2D ^{13}C–^{13}C DARR NMR spectra of (Ile, Thr)-^{13}C labeled MscL (Figs. S3 and S4), and partial chemical shift characterization of (Ile, Thr)-^{13}C labeled MscL (Tables S1 and S2).

Supplementary data associated with this article can be found, in the online version, at doi:10.1016/j.jmr.2010.02.003.

References

[1] F. Castellani, B. Van Rossum, A. Diehl, M. Schubert, K. Rehbein, H. Oschkinat, Structure of a protein determined by solid-state magic-angle-spinning NMR spectroscopy, Nature 420 (2002) 98–102.
[2] A. Loquet, B. Bardiaux, C. Gardiennet, C. Blanchet, M. Baldus, M. Nilges, T. Malliavin, A. Bockmann, 3D structure determination of the Crh protein from highly ambiguous solid-state NMR restraints, J. Am. Chem. Soc. 130 (2008) 3579–3589.
[3] L.J. Sperling, A.J. Nieuwkoop, A.S. Lipton, D.A. Berthold, C.M. Rienstra, High resolution NMR spectroscopy of nanocrystalline proteins at ultra-high magnetic field, J Biomol NMR 46 (2010) 149–155.
[4] A. Goldbourt, L.A. Day, A.E. McDermott, Assignment of congested NMR spectra: carbonyl backbone enrichment via the Entner–Doudoroff pathway, J. Magn. Reson. 189 (2007) 157–165.
[5] H. Heise, Solid-state NMR spectroscopy of amyloid proteins, ChemBioChem 9 (2008) 179–189.
[6] A. Lange, Z. Gattin, H. Van Melckebeke, C. Wasmer, A. Soragni, W.F. van Gunsteren, B.H. Meier, A combined solid-state NMR and MD characterization of the stability and dynamics of the HET-s(218–289) prion in its amyloid conformation, ChemBioChem 10 (2009) 1657–1665.
[7] S. Sun, A. Siglin, J.C. Williams, T. Polenova, Solid-state and solution NMR studies of the CAP-Gly domain of mammalian dynactin and its interaction with microtubules, J. Am. Chem. Soc. 131 (2009) 10113–10126.
[8] M. Hiller, L. Krabben, K.R. Vinothkumar, F. Castellani, B.J. Van Rossum, W. Kuhlbrandt, H. Oschkinat, Solid-state magic-angle spinning NMR of outer-membrane protein G from Escherichia coli, ChemBioChem 6 (2005) 1679–1684.
[9] A. Lange, K. Giller, S. Hornig, M.F. Martin-Eauclaire, O. Pongs, S. Becker, M. Baldus, Toxin-induced conformational changes in a potassium channel revealed by solid-state NMR, Nature 440 (2006) 959–962.
[10] H.L. Frericks, D.H. Zhou, L.L. Yap, R.B. Gennis, C.M. Rienstra, Magic-angle spinning solid-state NMR of a 144 kDa membrane protein complex: E. coli cytochrome bo3 oxidase, J. Biomol. NMR 36 (2006) 55–71.
[11] Y. Li, D.A. Berthold, H.L. Frericks, R.B. Gennis, C.M. Rienstra, Partial (13)C and (15)N chemical-shift assignments of the disulfide-bond-forming enzyme DsbB by 3D magic-angle spinning NMR spectroscopy, ChemBioChem 8 (2007) 434–442.
[12] S. Ganapathy, A.J. van Gammeren, F.B. Hulsbergen, H.J.M. de Groot, Probing secondary, tertiary, and quaternary structure along with protein-cofactor interactions for a helical transmembrane protein complex through 1H spin diffusion with MAS NMR spectroscopy, J. Am. Chem. Soc. 129 (2007) 1504–1505.
[13] M. Etzkorn, S. Martell, O.C. Andronesi, K. Seidel, M. Engelhard, M. Baldus, Secondary structure, dynamics, and topology of a seven-helix receptor in native membranes, studied by solid-state NMR spectroscopy, Angew. Chem. Int. Ed. Engl. 46 (2007) 459–462.
[14] S.D. Cady, T.V. Mishanina, M. Hong, Structure of amantadine-bound M2 transmembrane peptide of influenza A in lipid bilayers from magic-angle-spinning solid-state NMR: the role of Ser31 in amantadine binding, J. Mol. Biol. 385 (2009) 1127–1141.
[15] L. Shi, M.A. Ahmed, W. Zhang, G. Whited, L.S. Brown, V. Ladizhansky, Three-dimensional solid-state NMR study of a seven-helical integral membrane proton pump–structural insights, J. Mol. Biol. 386 (2009) 1078–1093.
[16] M. Hong, Determination of multiple-torsion angles in proteins by selective and extensive 13C labeling and two-dimensional solid-state NMR, J. Magn. Reson. 139 (1999) 389–401.
[17] M. Hiller, V.A. Higman, S. Jehle, B.J. van Rossum, W. Kuhlbrandt, H. Oschkinat, [2,3-(13)C]-labeling of aromatic residues-getting a head start in the magic-angle-spinning NMR assignment of membrane proteins, J. Am. Chem. Soc. 130 (2008) 408–409.

[18] K. Ozawa, P.S. Wu, N.E. Dixon, G. Otting, N-Labelled proteins by cell-free protein synthesis. Strategies for high-throughput NMR studies of proteins and protein-ligand complexes, FEBS J. 273 (2006) 4154–4159.
[19] I. Lehner, D. Basting, B. Meyer, W. Haase, T. Manolikas, C. Kaiser, M. Karas, C. Glaubitz, The key residue for substrate transport (Glu14) in the EmrE dimer is asymmetric, J. Biol. Chem. 283 (2008) 3281–3288.
[20] S. Sobhanifar, S. Reckel, F. Junge, D. Schwarz, L. Kai, M. Karbyshev, F. Lohr, F. Bernhard, V. Dotsch, Cell-free expression and stable isotope labelling strategies for membrane proteins, J Biomol NMR 46 (2010) 33–43.
[21] H.J. Kim, S.C. Howell, W.D. Van Horn, Y.H. Jeon, C.R. Sanders, Recent advances in the application of solution NMR spectroscopy to multi-span integral membrane proteins, Prog. Nucl. Magn. Reson. Spectrosc. 55 (2009) 335–360.
[22] G. Chang, R.H. Spencer, A.T. Lee, M.T. Barclay, D.C. Rees, Structure of the MscL homolog from Mycobacterium tuberculosis: a gated mechanosensitive ion channel, Science 282 (1998) 2220–2226.
[23] A.M. Powl, J.M. East, A.G. Lee, Importance of direct interactions with lipids for the function of the mechanosensitive channel MscL, Biochemistry 47 (2008) 12175–12184.
[24] Z. Liu, C.S. Gandhi, D.C. Rees, Structure of a tetrameric MscL in an expanded intermediate state, Nature 461 (2009) 120–124.
[25] C. Berrier, K.H. Park, S. Abes, A. Bibonne, J.M. Betton, A. Ghazi, Cell-free synthesis of a functional ion channel in the absence of a membrane and in the presence of detergent, Biochemistry 43 (2004) 12585–12591.
[26] E. Perozo, D.M. Cortes, P. Sompornpisut, A. Kloda, B. Martinac, Open channel structure of MscL and the gating mechanism of mechanosensitive channels, Nature 418 (2002) 942–948.
[27] K. Takegoshi, S. Nakamura, T. Terao, 13C–1H dipolar-assisted rotational resonance in magic-angle spinning NMR, Chem. Phys. Lett. 344 (2001) 631–637.
[28] Y. Li, R. Wray, C. Eaton, P. Blount, An open-pore structure of the mechanosensitive channel MscL derived by determining transmembrane domain interactions upon gating, FEBS J. 23 (2009) 2197–2204.
[29] H. Valadie, J.J. Lacapere, Y.H. Sanejouand, C. Etchebest, Dynamical properties of the MscL of Escherichia coli: a normal mode analysis, J. Mol. Biol. 332 (2003) 657–674.
[30] Y. Shen, A. Bax, Protein backbone chemical shifts predicted from searching a database for torsion angle and sequence homology, J. Biomol. NMR 38 (2007) 289–302.
[31] M.J. Sweredoski, K.J. Donovan, B.D. Nguyen, A.J. Shaka, P. Baldi, Minimizing the overlap problem in protein NMR: a computational framework for precision amino acid labeling, Bioinformatics 23 (2007) 2829–2835.
[32] D. Levy, A. Bluzat, M. Seigneuret, J.L. Rigaud, A systematic study of liposome and proteoliposome reconstitution involving Bio-Bead-mediated Triton X-100 removal, Biochim. Biophys. Acta 1025 (1990) 179–190.
[33] G. Rouser, S. Fkeischer, A. Yamamoto, Two dimensional then layer chromatographic separation of polar lipids and determination of phospholipids by phosphorus analysis of spots, Lipids 5 (1970) 494–496.
[34] C.R. Morcombe, K.W. Zilm, Chemical shift referencing in MAS solid state NMR, J. Magn. Reson. 162 (2003) 479–486.
[35] N.M. Szeverenyi, M.J. Sullivan, G.E. Maciel, Observation of spin exchange by two-dimensional Fourier transform 13C cross polarization-magic-angle spinning, J. Magn. Reson. 47 (1982) 462–475.
[36] A. Grommek, B.H. Meier, M. Ernst, Distance information from proton-driven spin diffusion under MAS, Chem. Phys. Lett. 427 (2006) 404–409.
[37] F. Delaglio, S. Grzesiek, G.W. Vuister, G. Zhu, J. Pfeifer, A. Bax, NMRPipe: a multidimensional spectral processing system based on UNIX pipes, J. Biomol. NMR 6 (1995) 277–293.

Supplementary data

Structural study of the membrane protein MscL using cell-free expression and solid-state NMR

Alaa Abdine, Michiel A. Verhoeven, Kyu-Ho Park, Alexandre Ghazi, Eric Guittet, Catherine Berrier, Carine Van Heijenoort and Dror E. Warschawski*

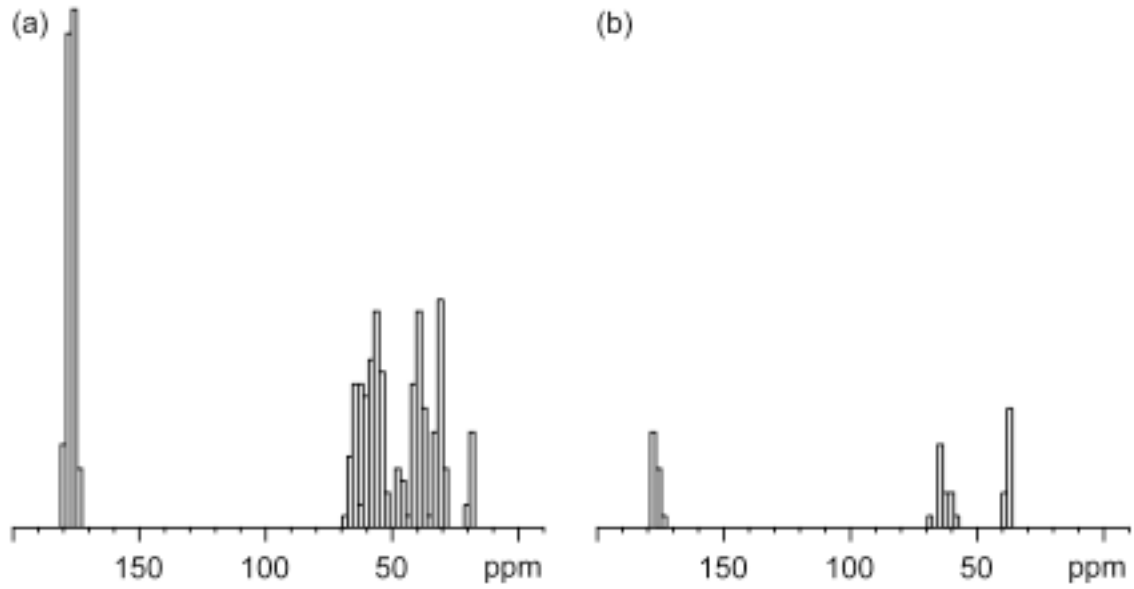

Figure S1. ^{13}C C', Cα and Cβ chemical shift simulations using SPARTA of a truncated *E. coli* MscL homology model based on the *M. tuberculosis* MscL X-ray structure and obtained after MD simulation: (a) U-^{13}C,^{15}N labeled and (b) (Ile, Thr)-^{13}C,^{15}N labeled. The chemical shift values are a weighted average of 6 independent pentameric MscL molecules, hence 30 monomers. Resonances from DOPC and spinning side bands appear in the spectra, not in the simulations.

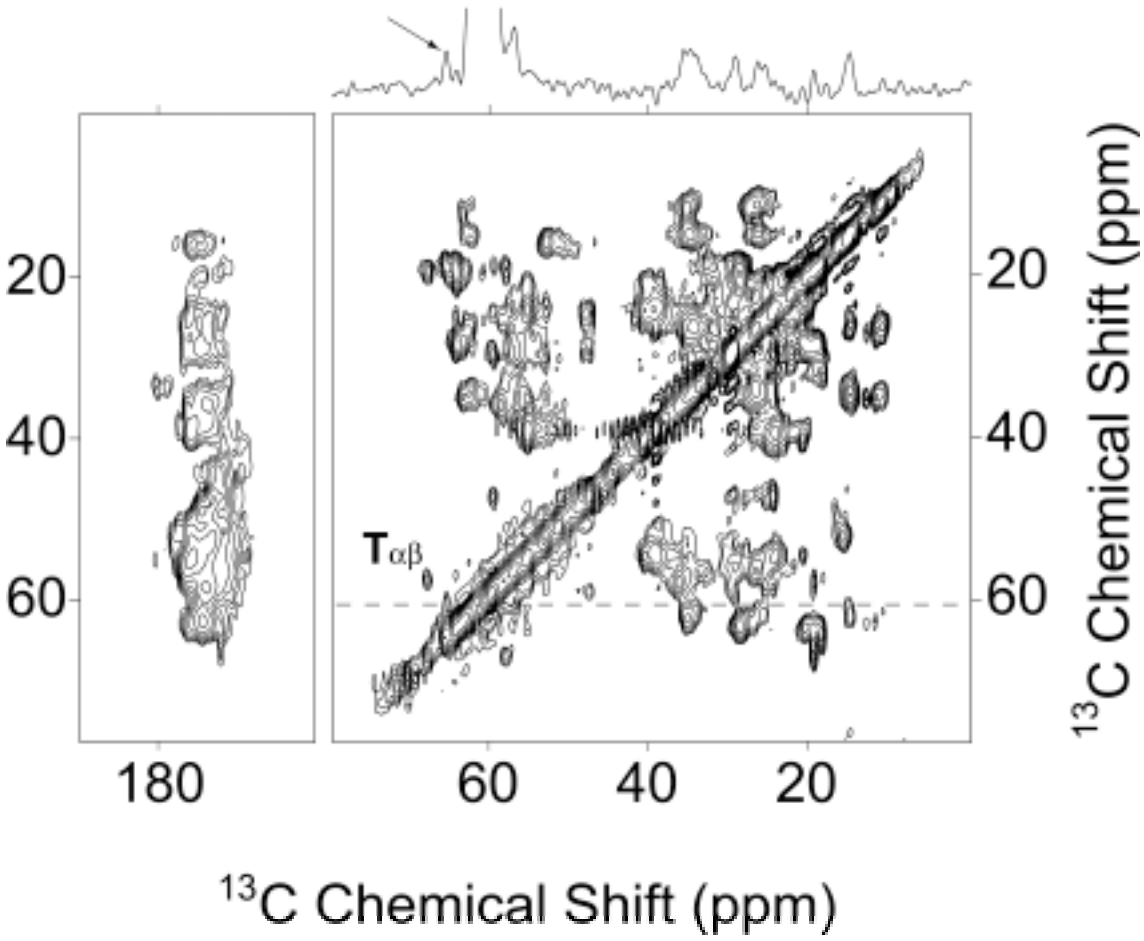

Figure S2. 2D ^{13}C-^{13}C PDSD NMR (20 ms mixing time, total experiment time: 56 hours) spectra of U-^{13}C,^{15}N labeled MscL/DOPC. In the case of the uniformly labeled protein, 256 scans per row are necessary to be able to observe the individual threonine cross signals, which are narrow, as can be seen on the cross section shown on top. The arrow indicates a threonine cross signal which is 120 Hz wide (0.68 ppm).

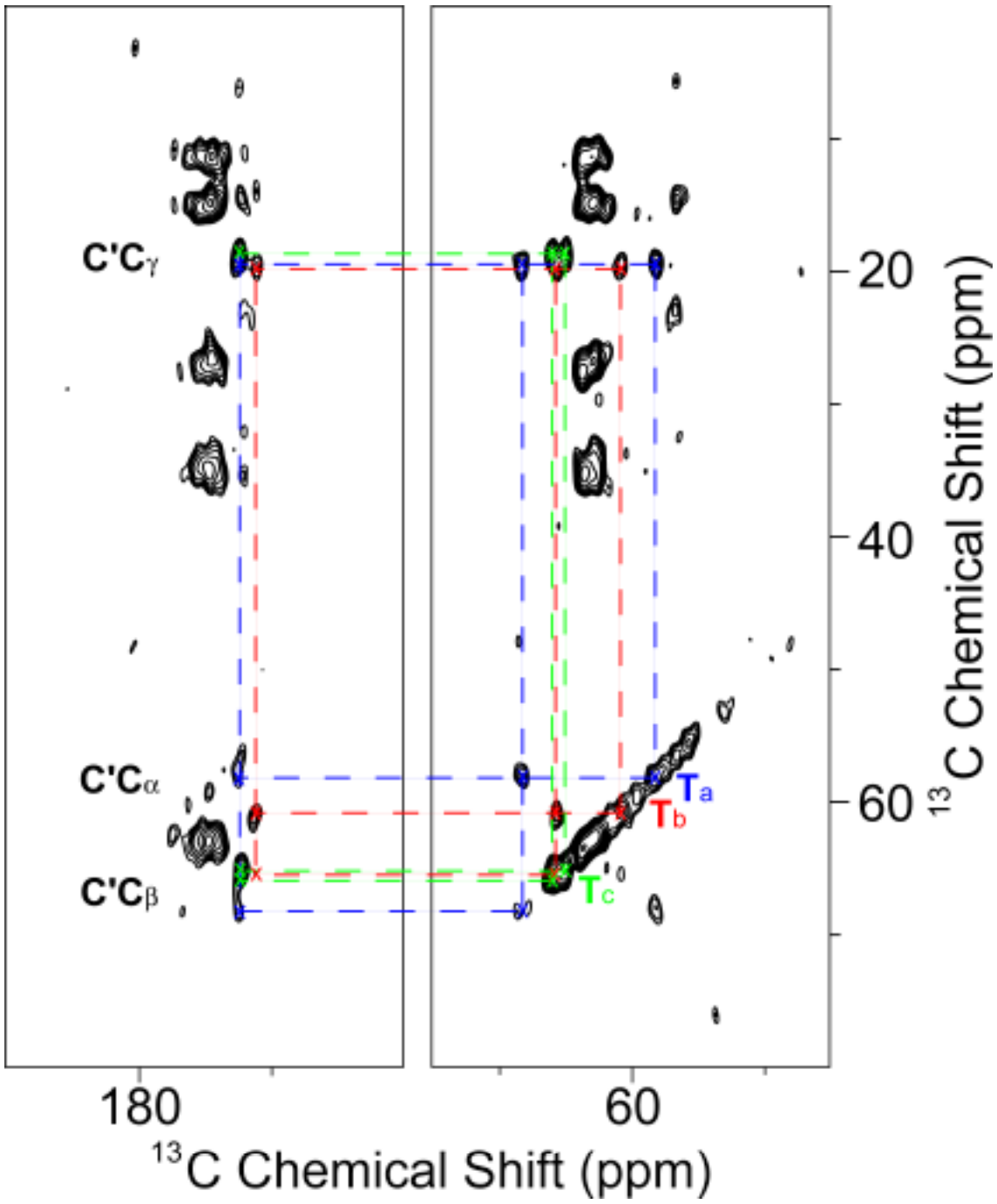

Figure S3. Magnifications of the 2D ^{13}C-^{13}C DARR NMR (100 ms mixing time, 56 hours of acquisition) spectrum of (Ile, Thr)-^{13}C,^{15}N labeled MscL/DOPC relevant for the characterization of the 3 Thr residue spin systems in MscL.

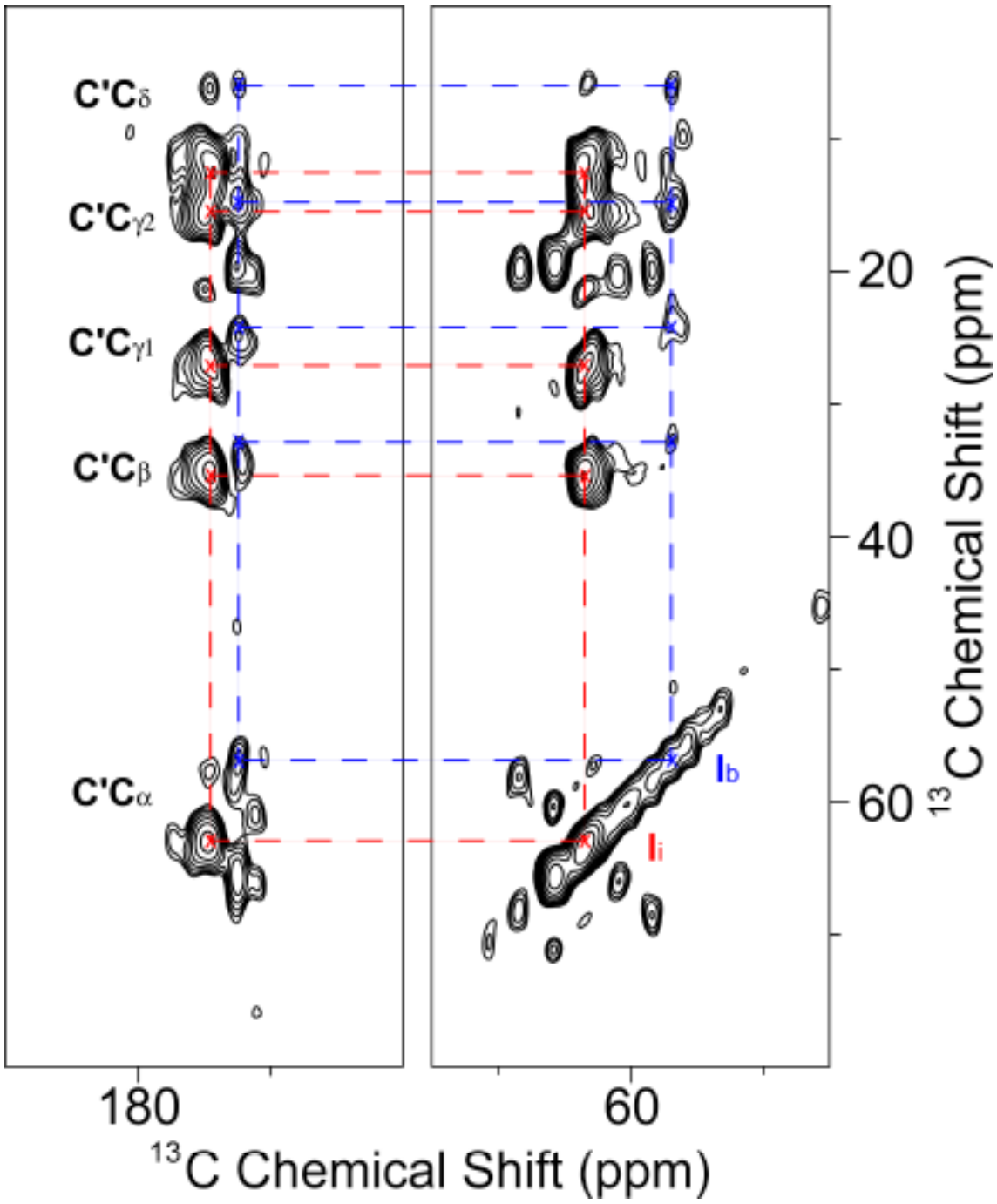

Figure S4. Magnifications of the 2D ^{13}C-^{13}C DARR NMR (200 ms mixing time, 14 hours of acquisition) spectrum of (Ile, Thr)-^{13}C,^{15}N labeled MscL/DOPC relevant for the characterization of the Ile residue spin systems in MscL. Only the spin system for Ib and Ii are shown here.

Table S1. Partial chemical shift characterization of threonine residues in (Ile, Thr)-$^{13}C/^{15}N$ labeled MscL. Peaks were picked from a series of spectra with several DARR mixing times (50, 100, 200, 500 ms) and the error is indicated as well. Since no sequential assignment was made, the amino acids were given an arbitrary alphabetic label. # indicates the number of cross peaks observed and used for the characterization.

amino acid		**C'**	**Cα**	**Cβ**	**Cγ**
Ta	shift (ppm)	172.3	58.2	68.3	19.6
	error (ppm)	0.2	0.3	0.2	0.2
	#	19	21	22	20
Tb		170.9	60.7	65.7	19.9
		0.2	0.2	0.2	0.2
		15	22	27	20
Tc		171.7	64.9	65.8	18.5
		0.2	0.1	0.1	0.1
		5	7	7	9

Table S2. Partial chemical shift characterization of isoleucine residues in (Ile, Thr)-$^{13}C/^{15}N$ labeled MscL. Peaks were picked from a series of spectra with several DARR mixing times (50, 100, 200, 500 ms) and the error is indicated as well. Since no sequential assignment was made, the amino acids were given an arbitrary alphabetic label. # indicates the number of cross peaks observed and used for the characterization.

amino acid		**C'**	**Cα**	**Cβ**	**Cγ1**	**Cγ2**	**Cδ**
Ia	shift (ppm)	172.2	55.9	35.0	24.1	14.3	9.9
	error (ppm)	0.2	0.1	-	0.1	-	0.1
	#	5	5	1	2	1	2
Ib		171.8	56.7	32.5	23.0	14.7	6.0
		0.3	0.1	0.2	0.2	0.3	0.3
		6	13	13	13	12	5
Ic		171.7	57.2	36.3	23.1	14.7	11.2
		-	0.1	-	0.2	-	-
		1	5	1	3	1	1
Id		172.5	58.5	36.2	27.1	15.6	11.7
		-	0.1	-	0.3	0.2	0.1
		1	3	1	2	3	2
Ie		174.3	59.1	36.0	26.4	15.6	12.0
		0.1	0.1	0.1	0.1	0.1	0.2
		3	6	2	2	3	2
If		-	60.2	34.9	-	15.5	-
		-	0.2	0.1	-	0.2	-
		-	4	3	-	3	-
Ig		175.1	60.8	33.7	26.6	15.4	10.8
		0.1	0.1	-	0.2	0.2	0.2
		2	4	1	3	3	3
Ih		174.7	62.5	33.9	26.4	14.6	10.9
		0.1	0.1	0.2	0.1	0.2	0.2
		6	10	9	9	9	5
Ii		175.2	63.5	35.3	27.7	14.9	12.0
		0.3	0.1	0.1	0.1	0.1	0.1
		5	7	7	7	7	7
Ij		171.7	65.4	36.0	28.3	-	12.3
		0.2	0.1	0.2	0.2	-	0.1
		3	3	2	3	-	3